AIAA AVIATION Forum
June 27-July 1, 2022, Chicago, IL & Virtual
AIAA AVIATION 2022 Forum

10.2514/6.2022-3962

A Comparative Study to Characterize the Effects of Adverse Weathers on the Flight Performance of an Unmanned-Aerial-System

Anvesh Dhulipalla[1], Nianhong Han[2], Haiyang Hu[3], Hui Hu[4],
Department of Aerospace Engineering, Iowa State University, Ames, Iowa, 50011

Abstract

There are very few experimental projects related to unmanned aerial vehicle performances under adverse weather conditions, which refer to any weather event which increases the risk of having an accident. The primary objective of this research is to experimentally study the flight performance of an Unmanned Aerial Vehicle (UAV) under windy, icing conditions by using the data acquired through onboard sensors. The experimental study was conducted in authorized airspace near Boone, IA. A quadcopter was utilized for this research, and all the test flights were fully autonomous between takeoff and landing. The experimental portion of the flight has fixed geolocation and trajectories in the designed missions. The variations in Unmanned Aerial System (UAS) power consumption were investigated during a fixed loiter time. It was found that the ice accreted on the propeller reflects glaze ice's complex characteristics. The glaze ice changes the shape of the leading edge and is very irregular. This transformation in aerodynamic shape greatly affects the lift and drag characteristics of the airfoil, thereby reducing the propeller's efficiency. The measurement results of the atmospheric parameters were also correlated with the UAS altitude data and power consumption data to elucidate the underlying physics for a better understanding of the effects of adverse weather on flight performances. The findings derived from this study are believed to be essential and helpful in elucidating the understanding of the energy consumption of drones due to icing and wind variations.

I. Introduction

The aviation routine weather report (METAR) and automated weather stations of various types report current ceiling information and additional weather data [1]. As technology advances, unmanned aerial vehicle systems are being deployed in the airspace, integrating various meteorological models to ensure the safety of people and infrastructure on the ground and flight systems. Due to the integration of innovative sensors and the development of advanced flight modes, the applications of UAS have been increasing. According to statistics, most aircraft accidents are due to poor atmospheric conditions. Wind resulting in aerial accidents was mainly divided into downburst, turbulent wind, wind shear, and wake vortex. Since UAVs operate at low Reynolds numbers, the selection of propellers and the Reynolds number drastically affect UAS performance. Brandt et al. tested propeller diameters ranging from 9-11 inches by fixing the rpm and changing the wind tunnel speed. The results revealed strong Reynolds number impacts, with lower RPMs causing performance decrease [2]. Due to their usage in lower altitudes, low flight speed, and fewer takeoff weights, they are more susceptible to wind disturbance than a manned aircraft. The turbulent flow may cause fluctuations resulting in unstable flight, and the wind shear will temporarily make UAV out of

[1] Graduate Research Assistant, Department of Aerospace Engineering.
[2] Graduate Research Assistant, Department of Aerospace Engineering.
[3] Graduate Research Assistant, Department of Aerospace Engineering.
[4] Martin C. Jischke Professor, Dept. of Aerospace Engineering, AIAA Associate Fellow. Email: huhui@iastate.edu

control [3]. Accurately assessing a UAV's attitude and position is the first step in precise control [4]. An alternative method of designing a guidance controller for UAVs under wind disturbances was developed to see the deviation from the assigned path [5]. Thrust, torque, motor speed, and electric power consumption of an isolated propeller and a full vehicle quadrotor under various climatic circumstances were compared, and in cold environments, Devices such as brushless motors and Electronic Speed Control (ESC) reduce cold environments' efficiency. It can be noted that as the altitude is increased, the required motor speed to achieve the reference thrust value increases. As the temperature is reduced, the thrust generated by the propeller increase [6]. To obtain the control of a fixed-wing UAV in a crosswind, an adaptive backstepping approach is designed by Brezoescu et al., [7]. The strategy was focused on reducing the position deviation of the airplane to a desired path in the lateral dynamics in the presence of unknown wind. The airplane is flown at a sideslip angle when aligned with the reference trajectory to maintain directional control. The influence of wind disturbances on the stability of six-rotor unmanned aerial vehicles (UAVs) was studied, with different disturbances in different orientations being evaluated. The obtained results reveal that the various rotor speeds are optimum to maintain stability after disturbances [8].

Aircraft icing occurs in clouds and during freezing rain in cold climatic regions. In general, the effects of in-flight ice accretion are harmful to flying. Because of the weight of the collected ice, aircraft become heavier. Irregular form changes can reduce lift forces. The more the surface area and form, the greater the drag. Ice on the propeller and engine parts can restrict thrust or air intake, resulting in a stall. Usually, aircraft icing is classified into rime, glaze, and mixed ice [9]. Rime Ice is generated when small, supercooled water droplets contact surfaces below freezing temperatures, less than -10^0 C. When supercooled water droplets reach the wing surface, they instantly freeze and maintain their hemispheric shape, generating a spear-like ice morphology on the leading edge. Glaze ice forms when temperatures are quite warm, between 0 to -10^0 C [10]. Water droplets have difficulty freezing on the wing surface in an environment with large water droplets, high liquid water content, and high airspeed. As a result, the droplets float along the surface until they are driven away by aerodynamic forces; otherwise, they will freeze. Unlike rime ice, this irregular shape may severely damage the flow field characteristics of the wing and cause lift loss, stall angle of attack decrease, and drag increase [11]. Extensive research has been performed on aerodynamic characteristics due to icing on the aircraft. The effects on aerodynamic performance and wake characteristics of a propeller model used for UAS under various icing conditions [12]. Compared with the no ice accretion case, rime ice accretion resulted in an increase of 15% in mean thrust force due to an increase in the effective chord length. While for glaze ice, there is a decrease in the mean value of thrust force by 70%. The propeller model consistently consumed more power despite varied ice accumulation over the propeller blades [13]. Ice shedding during flights can affect the performance of the system. The thrust fluctuations rose dramatically when ice shedding, potentially posing a flying safety hazard [14]. The thermal conductivity of the frame also plays an important role in ice accretion [15]. In a study by Hann et al., FENSAP-ICE was used to produce ice shapes on an airfoil and model the effects of aerodynamic icing on lift and drag at various angles of attack (AOA). Here a conclusion is drawn that icing at very low temperatures (rime) and very close to freezing temperatures (glaze) is less risky to a UAV than ice at intermediately low temperatures (mixed). The geometry of the ice shape also plays an important role in performance degradation [16]. A transition from rime-like to glaze-like behavior occurred for rising velocities in mixed ice conditions. During the changeover phase, enormous ice horn characteristics appeared, along with a significant drop in aerodynamic performance [17] [18]. On the NACA 0012 wing, high-speed videography of ice buildup was captured. The images are then digitized to extract the quantitative measurements. The roughness of the ice characteristics at the leading edge increases as the leading-edge ice develops and evolves. Previous research has demonstrated that due to unstable stagnation points at the leading-edge, 3D disturbances are created at low Mach numbers in glaze ice circumstances. Larger rivulets result in reduced aerodynamic performance. In the absence of freezing conditions, rivulet development occurs at lower wind speeds [19], demonstrating that rivulet width reduces with increasing wind speed [20].

The next step in this research is integrating an anti-/de-icing system. Current Anti-Icing/De-Icing methods are mainly thermal-based systems, i.e., use electrical heating or hot-air injection to heat massive

surfaces of wind turbine blades, which are inefficient and energy-consuming. A hybrid anti-/de-icing technology by integrating the minimized surface heating to delaminate ice accretion in critical regions and hydro-/ice-phobic coatings with ultra-low ice adhesion strength and outstanding mechanical durability to reject ice accretion and water run back over the surfaces of the turbine blades was introduced by Gao et al., [21].With a superhydrophobic coating, there is a reduction in power consumption during the glaze ice experiment. This improves the efficiency of UAS operations.

The vibration should also be considered when selecting and mounting electronic components on the frame. Verbeke et al. studied the main vibration sources impacting the UAV [22]. Ghalamchi et al., Pan et al. Analyzed the vibration due to the propeller. The motor/propeller pair is a major point of mechanical failure for such systems, with potential reasons for failure including mechanical wear of the motor bearing or damage to the propellers [23], [24].

Due to the extremely harsh weather conditions, limited experimental research was conducted on drones' icing and wind effects. In this research, we conducted an experimental investigation on the ice structure of the UAV Propellers and how different wind speeds affect the drones in real-time. The experimental investigation was conducted in an authorized air space at Agricultural Engineering and Agronomy Research Farm, in Boone, IA. The findings derived from this study are believed to be essential and helpful in elucidating the understanding of the energy consumption of drones due to icing and wind variations.

II. Internal Components and Experimental Setup

A. Avionics

Pixhawk 4 **Error! Reference source not found.** is an open-source flight controller running PX4 FMU (Flight management unit) software. PX4-based systems use sensors to determine vehicle state (needed for stabilization and to enable autonomous control). The vehicle states include position/altitude, heading, speed, airspeed, orientation (attitude), rotation rates in different directions, and battery level. The system requires a gyroscope, accelerometer, magnetometer (compass), and barometer. A GPS or other positioning system is needed to enable all automatic modes and some assisted modes. All the controllers, such as electronic speed controllers and servos, are connected via pulse width modulation to the controller board.

B. Propulsion:

The electric brushless DC motors are used as the powerplant for the quadcopter. The Readytosky motors are used. They are high torque 190 g, 920 Kv motors working with a 40A ESC, DJI 9-inch propellers. During windy or extreme icing events, a high discharge rate of 120C will be helpful for power requirements. A 5200mAh battery is chosen for the aircraft to provide the required rpm for all four motors, as shown in Figure 1.

Figure 1. LIPO battery(left), 9" propeller (4pcs), 920 kv Brushless DC motor (4pcs)

C. Communication and tracking

For long-range control of the UAS from a computer-based ground control station, the radio module is used Figure 2. It has an approximate range of 450 m. The telemetry and control of the aircraft are both communicated via the radio frequency distribution. We can control the UAS by a ground control station that runs QgroundControl software. The GPS module provides the navigation, altitude, and ground speed data of the UAV. It is equipped with an LED indicator and a safety switch.

(a) Telemetry Device (b) GPS

Figure 2. (a) RFD 915 MHz telemetry, (b) GPS Module.

Selecting the time to fly is the important criterion in this research; in contrast to rainy, windy, or snowy weather, non-icing weather is safer and easier to fly in. The aircraft will encounter less drag without strong winds, necessitating a faster takeoff and landing ground speed and distance. Power usage is less affected during non-icing weather than during extreme weather. The ground station runs on QGroundControl software, which provides full flight control and mission planning for drones. All wind flight experiments' loiter time and altitude have been fixed at 2 minutes at an altitude of 100 meters. After all the connections have been established, we must ensure the drone is ready to fly. To achieve that, we need to calibrate the quadcopter's magnetometer, gyroscope, and compass. During the quadcopter assembly, as shown in Figure 3, the orientation of the battery and the placement of internal components play an important role in vibration metrics.

Figure 3. Assembled Quadcopter after Calibration.

Since the drones fly at low altitudes, the icing occurs only if there is a freezing rain condition with low altitude cloud cover. It is necessary to be precautious during the flight because of low visibility. For a comparative study, flights conducted on non-icing days can be compared with flights conducted on windy, snowy, icing, and windy days. After the landing, the iced propellers were transferred using an insulating

foam box containing dry ice to a cooling chamber, where the propellers were carefully removed, and spray-painted. The 3D model is then analyzed using a 3D scanning technique based on Digital Image Processing (DIP), with one camera substituted by a laser projector to accurately capture the icing characteristics of the propeller blade. This was necessary to prevent laser light distortions from the 3D scanner through clear ice causing incorrect projections. The 3D scanning was performed using the apparatus shown in Figure 4. The model was placed on a rotating turntable and 120 2D scans were taken at an angle of 3º each, following which they were then fused to form a 3D object. This fused 3D object gave a qualitative representation of what the ice accretion looks like in different cases. The mass and volume of the collected ice were investigated for further analysis. On the stand, the lower side of the blade was not scanned since it was used to fix the propeller in the dry ice insulation box damaging the icing.

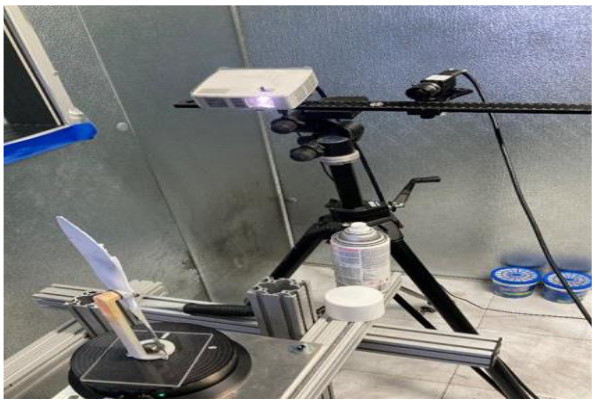

Figure 4. Experiment set up for 3D ice structure scanning.

III. Measurement Results and Discussions

A) Icing condition flight

As the weather conditions for Icing are freezing rain with low altitude cloud cover, we monitored the weather during the winter in Iowa for a chance of ice formation on the drone. On March 15^{th,} 2022, the weather was ideal for an icing flight with a temperature of $-3℃$, wind speed of 3 miles per hour (mph), 93% humidity, with a foggy cloud condition. These conditions are ideal for a glaze ice formation on the surfaces. As the ice accumulated during the flight, the battery was consumed rapidly, resulting in a pilot intervention to manually override the mission to return to the launch point. The iced Propeller in Figure 5 is then post-processed for further analysis, and Figure 6 shows the three-dimensional scanning results. The mass of ice accumulated is found to be 0.4859 g. Propeller has no ice shedding, and the formed ice structure reflects glaze ice's complex characteristics.

Because the ambient temperature was not low enough to consume all the latent heat of fusion at the moment of the impact of the supercooled water droplets, only a part of the supercooled water solidified into ice upon impact, and a large part of the water remained liquid after the impact and continued to stay on the blades surface or the ice surface and moved under aerodynamic force and centrifugal force until it finally froze into ice. Due to the flow of the boundary layer, the water droplets on the surface of the blade were driven by aerodynamic forces to move along the chord direction to the trailing edge, which expanded the area covered by the ice on the leading edge to the rear. At the same time, affected by the rotational movement, the water droplets did centrifugal movement outward along the spanwise direction, which made the ice on the leading edge continue to grow outward along the span direction, beyond the wingtip to grow into the airflow, as shown in Figure 5, Figure 6. This phenomenon can also be seen from the cross-sectional view of the scanned 3D objects in Figure 7 that the glaze ice changes the shape of the leading edge and is very irregular. This transformation in aerodynamic shape greatly affects the lift and drag characteristics of the airfoil, thereby reducing the propeller’s efficiency.

(a) Photograph of suction Side of the propeller.

(b) Photograph of pressure side of the propeller.

Figure 5. Formation of sharp-edged glaze ice on the suction side (a) and Pressure side (b) of the propeller.

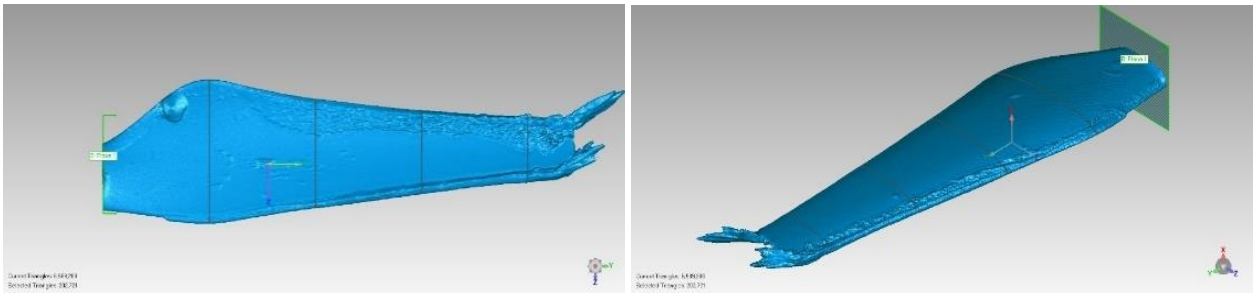

Figure 6. 3D Image of the cross-section position and glaze ice formation.

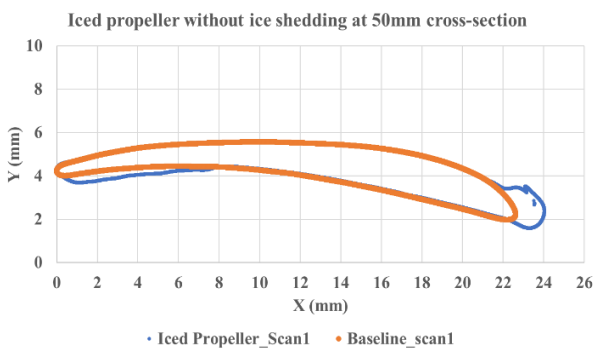

(a) Cross sectional profile at 50 mm.

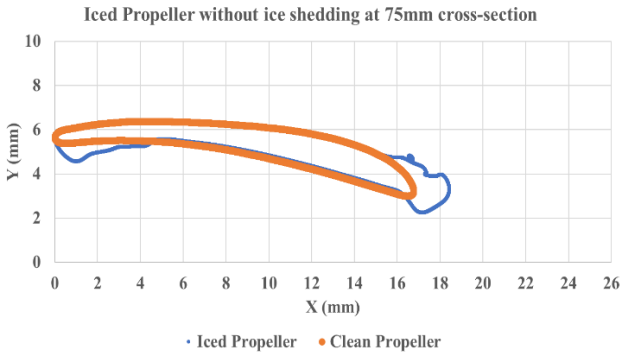

(b) Cross sectional profile at 75 mm.

Figure 7. change in aerodynamic shape observed by cross-sectional profiles of propeller without ice shedding, before and after icing with distance from a center plane at (a) 50mm (b)75mm.

Ice shedding will occur when the structural strength of ice is insufficient to support the combination of aerodynamic force, centrifugal force, ice, and propeller contact surface stress [13]. Figure 8 shows the

propeller with ice shedding, and Figure 9 shows the three-dimensional scanning results, and the mass of ice accumulated is found to be 0.23173 g. As a result of this shedding, the ice in the falling component was likely to collide with other parts of the aircraft body. Furthermore, because the propeller is a spinning component, it is particularly sensitive to the structure's mass distribution, and additional structures such as ice cones would produce extra vibrations, compromising flight safety even though the ice accumulated on the propeller is less as shown by the cross-sectional view of the scanned 3D objects in Figure 10. Even a small change in shape affects the overall performance of the drone. However, the ice build-up continues, and if allowed for sufficient time, all aerodynamic lift forces could be reduced, leading to an ultimate crash.

Figure 8. Ice formation on the suction side of a propeller.

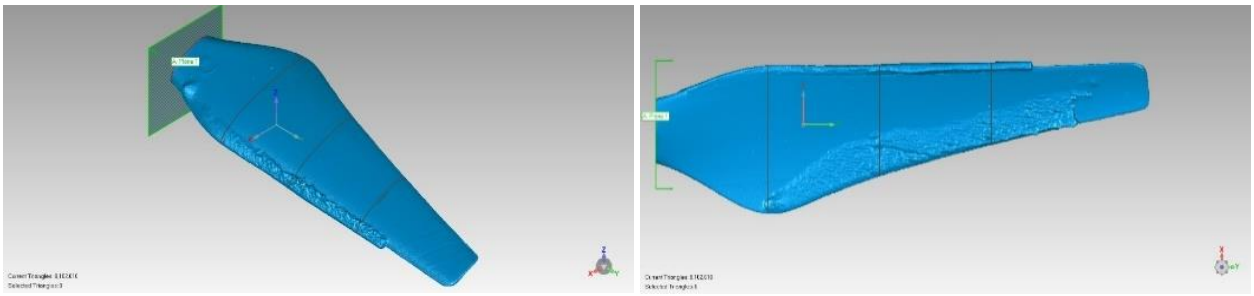

Figure 9. 3D Image of the cross-section position of propeller with ice shedding.

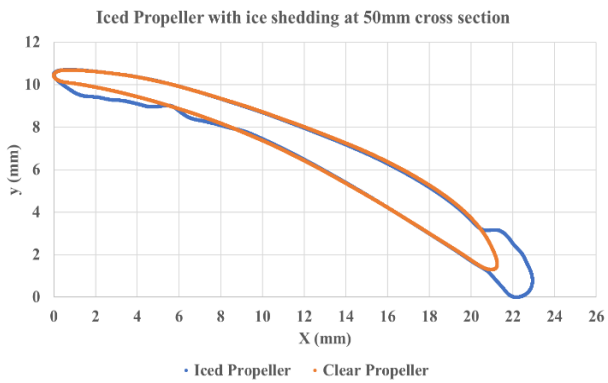

(a) Cross sectional profile at 50 mm

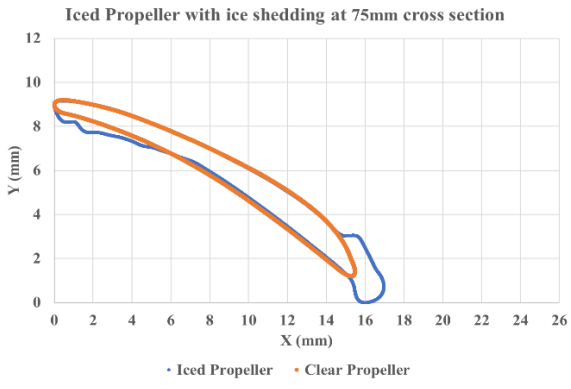

(b) Cross sectional profile at 75 mm

Figure 10. change in aerodynamic shape observed by cross-sectional profiles of propeller with ice shedding, before and after icing with distance from a center plane at (a) 50mm (b)75mm.

In Figure 11, we can notice a continuous increase in power consumption during the entire loiter time of 80 seconds from 220 Watts to 830 Watts of the icing flight. The area under this plot results in the average energy consumed, which is 404 Joules. As the battery had reached a critical stage of around 130 seconds, the manual control was taken, making the drone land safely. During the descent, it can be observed that around 140 seconds, there is a sharp decrease in the amount of power consumed, and there is an increase in altitude in this region. This fluctuation in altitude is due to a sudden change in mass of about 0.25471 g due to ice shedding. To maintain the altitude, the autopilot (PID controller) has to reduce the throttle resulting in a decreased power consumption. The ice formation continues to happen until the drone has landed. For a comparative study, the power consumption of a non-icing weather flight is recorded as shown in Figure 11 (Top). It depicts that the amount of power consumed during loiter is constant at around 200 Watts, the area beneath the loiter time results in a total Energy consumed which is 204 Joules. Hence, the percentage increase in the energy consumed by icing flight compared to non-icing weather flight is 93%. The throttle controls the power provided to the aircraft to fly. In the case of electric motor-driven vehicles like a quadcopter, the current drawn is adjusted to accommodate the power requirements.

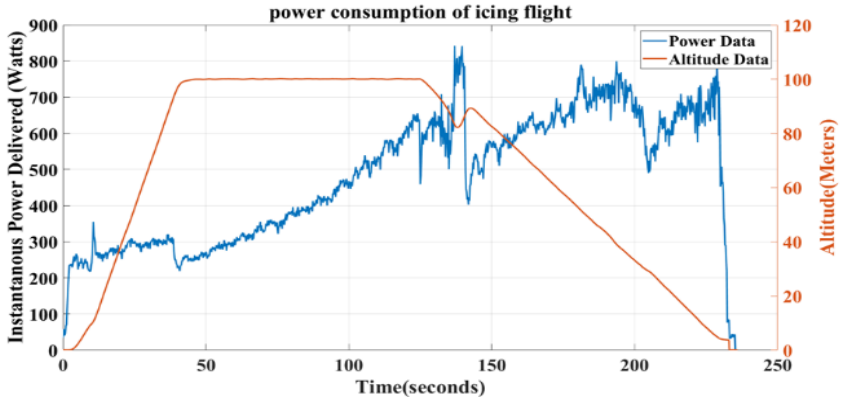

(a) Power consumption and altitude under an icing condition

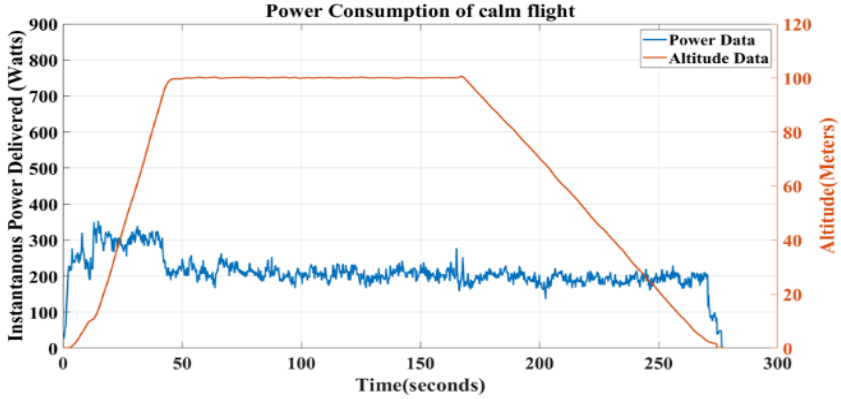

(b) Power consumption and altitude under a non-icing condition

Figure 11. Measured power consumption and flight altitude under different weather conditions.

B) Windy condition flight

The experimental loiters designed to collect the data. During the Windy flight experiment, the wind is variable, i.e., in different directions, and we have sudden gusts during the flight. The performance of UAS due to this effect is studied. Observing the loiters shows that the windy weather led to an unstable flight. Various experimental flights were performed over different wind and gust speeds, as shown in Table 1, and the average of the power consumed during the loitering was gathered and investigated. From Figure 12, cubic fitting with the polynomial expressions is plotted, and it is predicted that the power consumption increases with increased wind speed and gust speed.

Table 1. Experimental flights at different wind speeds

Date	Wind speed (mph)	Gust speed (mph)	Temperature °F	Humidity %
03/25/2022	7	0	46	87
04/11/2022	8	14	63	22
04/29/2022	19	21	61	100
04/12/2022	22	31	60	100
03/24/2022	26	36	45	39

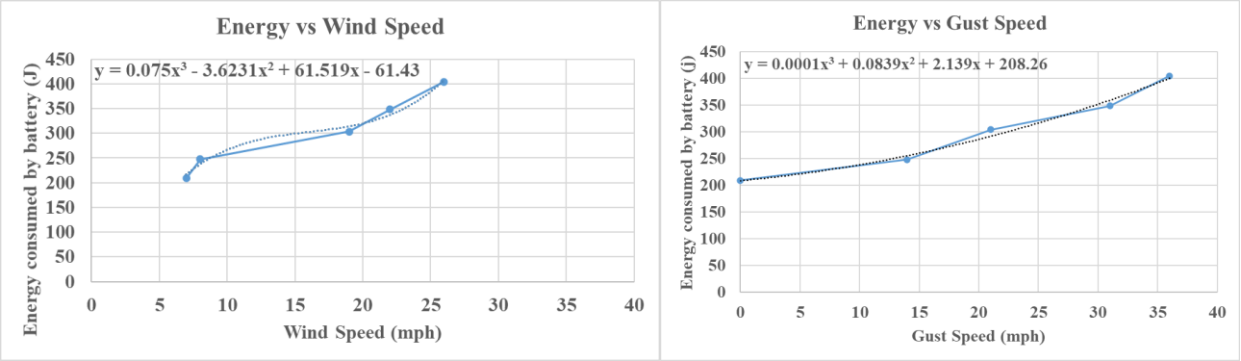

Figure 12.The plot of Energy consumed by the battery during loiter of different flights compared with wind speed (left) and gust speed (right)

When the low-speed weather condition is compared with high speed, an energy consumption increment is about 94%. Since the power consumption is increased by throttle control only, it is possible that this large amount would only trigger an increase in throttle while loitering at a fixed altitude under extreme flight conditions.

IV.Conclusion

This study provides the details of the experimental setup and procedures developed to investigate the negative effects of weather on the quadcopter. The meteorological conditions were studied, and flights were conducted in different weather conditions. The ice formation on the quadcopters' propellers was investigated, and the mass of ice accumulated on different propellers was noticed to be 0.23173 g and 0.4859 g. The difference in ice mass of 0.25471 g was concluded to be due to ice shedding.

This study confirms that by the application of 3D Scanning technology, iced propellers revealed the sharp horn like glaze ice formation on leading edge and the runback due to aerodynamic forces and

centrifugal forces were responsible for trailing edge Icing. The total energy consumed by icing flight is more by 98% when compared to non-icing weather flight. Comparing different propellers, the discarded ice mass was responsible for sudden spikes in power consumption. Falling ice mass may impact other parts of the drone resulting in a potential threat to flight safety.

The highest power was consumed during the icing condition during the experimental flights. The UAS consumed the second-largest amount of power during flight under strong winds, which is 94% when the highest wind speed flight is compared with a non-icing weather flight. Non-icing weather conditions led to the least amount of power consumption.

V.Future Work:

The flight test needs to be conducted under different weather conditions like Rain, Snow, Icing. In this investigation, clear (glaze) ice formation was investigated. Rime ice and mixed ice conditions may also be investigated in future studies. With the appropriate airspace authorizations, Beyond Visual Line of Sight (BVLOS) flights may be conducted at higher altitudes and longer ranges. Various comparisons lead to different results; all the data must be studied thoroughly for different weather conditions, and then comparing them with non-icing weather tells us the accuracy of the flight performance. Furthermore, the 3D scanned propellers can be 3D printed to analyze vibration, acoustics, and performance variations.

Acknowledgments

The research work is partially supported by Iowa Space Grant Consortium (ISGC) Base Program for Aircraft Icing Studies, National Science Foundation (NSF) under award numbers of CMMI- 1824840 and CBET- 1916380

References

[1] "Pilot's Handbook of Aeronautical Knowledge, 2016," *United States Department of Transportation -- Publications & Papers*, Jan. 2016, Accessed: Jan. 27, 2022. [Online]. Available: https://digitalcommons.unl.edu/usdot/66

[2] J. Brandt, M. S.-49th A. A. S. M. including, and undefined 2011, "Propeller performance data at low reynolds numbers," *arc.aiaa.org*, 2011, Accessed: Jan. 26, 2022. [Online]. Available: https://arc.aiaa.org/doi/abs/10.2514/6.2011-1255

[3] B. H. Wang, D. B. Wang, Z. A. Ali, B. Ting Ting, and H. Wang, "An overview of various kinds of wind effects on unmanned aerial vehicle," *Measurement and Control (United Kingdom)*, vol. 52, no. 7–8, pp. 731–739, Sep. 2019, doi: 10.1177/0020294019847688.

[4] C. Hajiyev, H. Ersin Soken, and S. Yenal Vural, "State Estimation and Control for Low-cost Unmanned Aerial Vehicles," *State Estimation and Control for Low-cost Unmanned Aerial Vehicles*, 2015, doi: 10.1007/978-3-319-16417-5.

[5] C. Liu, O. McAree, and W. H. Chen, "Path-following control for small fixed-wing unmanned aerial vehicles under wind disturbances," *International Journal of Robust and Nonlinear Control*, vol. 23, no. 15, pp. 1682–1698, Oct. 2013, doi: 10.1002/rnc.2938.

[6] M. Scanavino, A. Avi, A. Vilardi, and G. Guglieri, "Unmanned Aircraft Systems Performance in a Climate-Controlled Laboratory," *Journal of Intelligent and Robotic Systems: Theory and Applications*, vol. 102, no. 1, May 2021, doi: 10.1007/s10846-021-01392-4.

[7] A. Brezoescu, T. Espinoza, P. Castillo, and R. Lozano, "Adaptive trajectory following for a fixed-wing UAV in presence of crosswind," *Journal of Intelligent and Robotic Systems: Theory and Applications*, vol. 69, no. 1–4, pp. 257–271, Jan. 2013, doi: 10.1007/s10846-012-9756-8.

[8] X. Li, B. Zhao, Y. Yao, H. Wu, and Y. Liu, "Stability and Performance Analysis of Six-Rotor Unmanned Aerial Vehicles in Wind Disturbance," *Journal of Computational and Nonlinear Dynamics*, vol. 13, no. 3, Mar. 2018, doi: 10.1115/1.4038776/380673.

[9] R. Gent, N. Dart, J. C.-Phil. Trans. R. Soc. Lond. A, and undefined 2000, "Aircraft icing," *peter2000.co.uk*, vol. 358, no. 1776, pp. 2873–2911, 2000, doi: 10.1098/rsta.2000.0689.

[10] W. B. Wright, *User manual for the NASA Glenn ice accretion code LEWICE*. 2002. Accessed: Jan. 30, 2022. [Online]. Available: https://www.researchgate.net/profile/William-Wright-23/publication/24324761_User_Manual_for_the_NASA_Glenn_Ice_Accretion_Code_LEWICE/links/0c96051dc1c8013c73000000/User-Manual-for-the-NASA-Glenn-Ice-Accretion-Code-LEWICE.pdf

[11] M. P.-J. of aircraft and undefined 2000, "Predicting glaze or rime ice growth on airfoils," *arc.aiaa.org*, vol. 37, no. 1, pp. 117–121, 2000, doi: 10.2514/2.2570.

[12] Y. Liu, L. Li, W. Chen, W. Tian, and H. Hu, "An experimental study on the aerodynamic performance degradation of a UAS propeller model induced by ice accretion process," *Experimental Thermal and Fluid Science*, vol. 102, pp. 101–112, Apr. 2019, doi: 10.1016/j.expthermflusci.2018.11.008.

[13] Y. Liu, L. Li, Z. Ning, W. Tian, and H. Hu, "Experimental investigation on the dynamic icing process over a rotating propeller model," *Journal of Propulsion and Power*, vol. 34, no. 4, pp. 933–946, 2018, doi: 10.2514/1.B36748.

[14] N. Han, H. Hu, and H. Hu, "An Experimental Investigation on the Dynamic Ice Accretion Process over the Blade Surface of a Rotating UAV Propeller," Jan. 2022. doi: 10.2514/6.2022-1538.

[15] L. Li, Y. Liu, Z. Zhang, H. H.-I. J. of H. and Mass, and undefined 2019, "Effects of thermal conductivity of airframe substrate on the dynamic ice accretion process pertinent to UAS inflight icing phenomena," *aere.iastate.edu*, vol. 131, pp. 1184–1195, 2019, doi: 10.1016/j.ijheatmasstransfer.2018.11.132.

[16] R. Hann, A. Wenz, K. Gryte, and T. A. Johansen, "Impact of atmospheric icing on UAV aerodynamic performance," *2017 Workshop on Research, Education and Development of Unmanned Aerial Systems (RED-UAS)*, pp. 66–71, Nov. 2017, doi: 10.1109/RED-UAS.2017.8101645.

[17] R. Hann and T. A. Johansen, "UAV icing: the influence of airspeed and chord length on performance degradation," *Aircraft Engineering and Aerospace Technology*, vol. 93, no. 5, pp. 832–841, 2021, doi: 10.1108/AEAT-06-2020-0127.

[18] R. M. Waldman and H. Hu, "High-speed imaging to quantify the transient ice accretion process on a NACA 0012 airfoil," 2015. doi: 10.2514/6.2015-0033.

[19] K. Zhang, J. Blake, R. Alric, and H. Hu, "An experimental investigation on wind-driven rivulet/film flows over a NACA0012 airfoil by using digital image projection technique," 2014. doi: 10.2514/6.2014-0741.

[20] S. P. Otta and A. P. Rothmayer, "Instability of stagnation line icing," *Computers & Fluids*, vol. 38, no. 2, pp. 273–283, Feb. 2009, doi: 10.1016/J.COMPFLUID.2008.02.005.

[21] L. Gao, Y. Liu, L. Ma, and H. Hu, "A hybrid strategy combining minimized leading-edge electric-heating and superhydro-/ice-phobic surface coating for wind turbine icing mitigation," *Renewable Energy*, vol. 140, pp. 943–956, Sep. 2019, doi: 10.1016/j.renene.2019.03.112.

[22] J. Verbeke, K. U. Leuven, J. Verbeke, and S. Debruyne, "Vibration analysis of a UAV multirotor frame," *researchgate.net*, 2016, Accessed: Jan. 24, 2022. [Online]. Available: https://www.researchgate.net/profile/Jon-Verbeke/publication/313846241_Vibration_analysis_of_a_UAV_multirotor_frame/links/58aab653aca27206d9b99643/Vibration-analysis-of-a-UAV-multirotor-frame.pdf

[23] B. Ghalamchi, Z. Jia, and M. W. Mueller, "Real-Time Vibration-Based Propeller Fault Diagnosis for Multicopters," *IEEE/ASME Transactions on Mechatronics*, vol. 25, no. 1, pp. 395–405, Feb. 2020, doi: 10.1109/TMECH.2019.2947250.

[24] J. Pan, N. Farag, T. Lin, … R. J. the A. C. of the, and undefined 2002, "Propeller induced structural vibration through the thrust bearing," *acoustics.asn.au*, 2002, Accessed: Jan. 24, 2022. [Online]. Available: https://www.acoustics.asn.au/conference_proceedings/AAS2002/AAS2002/PDF/AUTHOR/AC020034.PDF